Dissociable contribution of prefrontal and striatal dopaminergic genes to learning in economic games

Eric Set[a,b], Ignacio Saez[a], Lusha Zhu[c], Daniel E. Houser[d], Noah Myung[e], Songfa Zhong[f], Richard P. Ebstein[g,1], Soo Hong Chew[f,1], and Ming Hsu[a,1]

[a]Haas School of Business and Helen Wills Neuroscience Institute, University of California, Berkeley, CA 94720; [b]Department of Economics, University of Illinois at Urbana–Champaign, Urbana, IL 61801; [c]Virginia Tech Carilion Research Institute, Roanoke, VA 24016; [d]Department of Economics and Interdisciplinary Center for Economics Science, George Mason University, Fairfax, VA 22030; [e]Graduate School of Business & Public Policy, Naval Postgraduate School, Monterey, CA 93943; and Departments of [g]Psychology and [f]Economics, National University of Singapore, Singapore 117570

Edited by Antonio Rangel, California Institute of Technology, Pasadena, CA, and accepted by the Editorial Board April 28, 2014 (received for review August 29, 2013)

Game theory describes strategic interactions where success of players' actions depends on those of coplayers. In humans, substantial progress has been made at the neural level in characterizing the dopaminergic and frontostriatal mechanisms mediating such behavior. Here we combined computational modeling of strategic learning with a pathway approach to characterize association of strategic behavior with variations in the dopamine pathway. Specifically, using gene-set analysis, we systematically examined contribution of different dopamine genes to variation in a multistrategy competitive game captured by (*i*) the degree players anticipate and respond to actions of others (belief learning) and (*ii*) the speed with which such adaptations take place (learning rate). We found that variation in genes that primarily regulate prefrontal dopamine clearance—catechol-*O*-methyl transferase (COMT) and two isoforms of monoamine oxidase—modulated degree of belief learning across individuals. In contrast, we did not find significant association for other genes in the dopamine pathway. Furthermore, variation in genes that primarily regulate striatal dopamine function—dopamine transporter and D2 receptors—was significantly associated with the learning rate. We found that this was also the case with COMT, but not for other dopaminergic genes. Together, these findings highlight dissociable roles of frontostriatal systems in strategic learning and support the notion that genetic variation, organized along specific pathways, forms an important source of variation in complex phenotypes such as strategic behavior.

neuroeconomics | experience-weighted attraction | eigenSNPs

Game theory describes strategic interactions where success of players' actions depends on those of coplayers and has been instrumental in the quantitative analysis of social behavior (1, 2). In humans, there is substantial evidence from laboratory experiments that, in addition to learning about rewards and punishments available in the environment, people also anticipate and respond to competitive or cooperative actions of other participants (1, 3). Specifically, learning in strategic settings can be parsimoniously characterized using two learning rules across a wide range of strategic contexts and experimental conditions: (*i*) reinforcement-based learning (RL) through trial and error and (*ii*) belief-based learning through anticipating and responding to the actions of others (1, 4).

Only in the past decade, however, have researchers begun to characterize the biological substrates underlying decision making in game theoretic settings (3). At the neural level, applications of functional neuroimaging, combined with formal mathematical models of behavior, have elucidated key roles of the frontostriatal circuits and putative dopaminergic mechanisms in guiding social behavior (5, 6). In particular, during competitive strategic interactions activity in the prefrontal cortex (PFC) was found to be better accounted for by models that incorporate higher-order inferences about opponents' behavior, rather than simpler forms of trial-and-error reinforcement learning (5, 7).

In comparison, despite the explosion in availability of genomic data as well as known heritability of economic behavior, we know much less about the molecular genetic underpinnings of the intermediate neural mechanisms (8, 9). Here we sought to shed light on the neurogenetic basis of strategic behavior by exploiting known variation in the set of genes within the dopamine pathway and studying their effects on behavior. A genetic pathway consists of a group of functionally related genes that mediate a particular biological process (e.g., dopamine functioning) (Fig. 1*B*) (10). For example, the DAT1 gene encodes the dopamine transporter (DAT), whose function is to remove dopamine from the synaptic cleft, thus terminating the signal of the neurotransmitter. Although these pathways are abstractions of complex biological processes that have no simple start or end points, they have been invaluable to researchers because they capture and organize our knowledge in a parsimonious and tractable manner (10).

Studying the molecular basis of social and strategic behavior in the context of economic games and specific biological pathways offers a number of important advantages. First, the dopamine pathway seems to play a fundamental role in social behavior in all known vertebrate species by virtue of its involvement in (social) reward and decision-making processes (11, 12). Unlike economic phenotypes such as wealth that are far removed from the proximate biological mechanisms, models of strategic learning provide highly parsimonious and mathematically rigorous descriptions of behavior and have been shown to have substantial predictive validity at both behavioral and neural levels (3, 9).

Significance

Game theory is used throughout the social and biological sciences to study behavior in social interactions. Recent research suggests an important role for the dopamine neurotransmitter system in these types of decisions. This study used a competitive game to study how people varied in their decision-making processes and related these differences in the set of genes that carry out biological functions required for dopaminergic functioning. We found that genes differentially expressed in separate brain regions influenced distinct components of people's decision-making processes and that a surprising degree of consistency exists with what is known at the brain level about how people make decisions in social interactions.

Author contributions: E.S., L.Z., S.Z., and M.H. designed research; E.S. performed research; E.S. and M.H. contributed new reagents/analytic tools; E.S., I.S., D.E.H., and M.H. analyzed data; and E.S., I.S., L.Z., D.E.H., N.M., S.Z., R.P.E., S.H.C., and M.H. wrote the paper.

The authors declare no conflict of interest.

This article is a PNAS Direct Submission. A.R. is a guest editor invited by the Editorial Board.

[1]To whom correspondence may be addressed. E-mail: rpebstein@gmail.com, ecscsh@nus.edu.sg, or mhsu@haas.berkeley.edu.

This article contains supporting information online at www.pnas.org/lookup/suppl/doi:10.1073/pnas.1316259111/-/DCSupplemental.

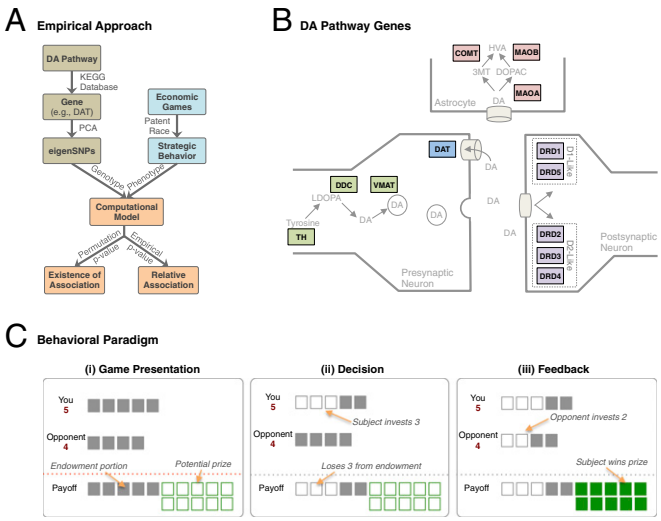

Fig. 1. (*A*) Starting with the Kyoto Encyclopedia of Genes and Genomes dopamine pathway, we selected a set of genes directly related to dopamine functioning (Table 1). For each gene, we took all available SNPs in the GWA dataset and conducted PCA to account for correlation due to LD. On the phenotype side, we used a laboratory-based economic game (patent race). These were then combined in our computational model, where parameters were estimated using maximum likelihood. Hypothesis testing was done using two different methods: (*i*) permutation *P* values under the null hypothesis of no association and (*ii*) empirical *P* values by comparing to randomly matched genes in the GWA dataset. (*B*) Dopamine pathway genes are represented in a stylized version of the dopamine synapse and include dopamine genes directly involved in synthesis (green), uptake (blue), and metabolism (pink) and receptors (violet). Certain details, such as presynaptic autoreceptors, have been omitted for clarity. (*C*) In the patent race, subjects were presented with (*i*) the game with information regarding their endowment, the endowment of the opponent, and the potential prize. (*ii*) Subjects inputted the decision (self-paced) by pressing a button mapped to the desired investment amount from the initial endowment. (*iii*) After a brief delay, the opponent's choice was revealed. If the subject's investment was strictly more than those of the opponent, the subject won the prize; otherwise, the subject lost the prize. In either case, the subject kept the portion of the endowment not invested.

Importantly, focusing on specific biological pathways allows us to exploit existing knowledge regarding the biological mechanisms underlying behavior, and in particular known relationships between gene and brain. The dopamine system is known to exhibit remarkable regional variation in expression levels of genes coding for the set of enzymes, receptors, and transporters involved in dopamine functioning (Fig. 1*C*) (11, 13). In the PFC, where DAT1 expression is low, genes regulating enzymatic breakdown, in particular catechol-*O*-methyl transferase (COMT) and to a lesser extent isoforms of the monoamine oxidase (MAO) genes, are important determinants of dopamine flux (14). In contrast, these genes have much less impact on striatal dopamine levels, where DAT1 expression is high (15). On the receptor side, regional variation results from distribution of dopamine receptor types (16). Receptors of the D1 family, D1 and D5, are expressed throughout the brain. In contrast, receptors in the D2 family exhibit more regional specificity: D2 receptors are expressed primarily in the dorsal striatum, D3 receptors in the ventral striatum, including nucleus accumbens but less so in dorsal striatum, and D4 receptors in the frontal cortex and limbic regions (16).

These differences have known important consequences for cognition and behavior (14, 15) but to our knowledge have not been explored in strategic or social behavior in humans. Here we studied the behavior of 218 participants in a multistrategy competitive game, the so-called patent race, in a stylized but well-characterized setting of a population with many anonymously interacting agents and low probability of re-encounter (Fig. 1*C* and *SI Materials and Methods*) (5).

Moreover, using this game, previous neuroimaging results have been able to disaggregate trial-by-trial variation in neural responses along frontostriatal circuits to distinct computational signatures of RL and belief learning processes (5). In particular, whereas the medial PFC was found to respond selectively to belief-based inputs and reflected individual differences in degree of engagement of belief learning, striatal activity was correlated with both reinforcement and belief-based signals, suggesting possible convergence of these signals in the striatum (5). Building upon these findings, therefore, we investigated (*i*) the degree to which variation in strategic learning can be captured by variation in genes in the dopamine pathway and (*ii*) the extent to which these variations are organized along dissociable prefrontal and striatal neural systems.

Consistent with our goal of capturing overall variation in dopamine functioning and its effects on strategic learning, we included not only exonic polymorphisms that exert direct effects on protein sequence and functions but also those in intronic and UTRs, as well as variable-number tandem repeats (VNTRs) and synonymous exonic polymorphisms (Fig. 1*B* and *SI Materials and Methods*). Although long thought to have no biological effect, intronic and synonymous mutations are now known to affect gene translational and transcriptional efficiencies, and consequently protein levels, as opposed to altering protein structure itself (17). To account for correlated regressors owing to linkage disequilibrium (LD), we took a dimension reduction approach and created a set of eigenSNPs using principal components analysis (PCA) (Fig. 1*B* and *Materials and Methods*). Compared with traditional candidate gene approaches, this multilocus approach can be used to detect association between a phenotype and groups of SNPs (genes) and is more efficient when there exist weaker but coordinated effects arising from multiple SNP markers (10).

Results

Model-Based Characterization of Behavior. To characterize individual variation in choice behavior, we adopted a hybrid model—experience weighted attraction (EWA)—that combines and nests both reinforcement and belief learning (1, 4). Specifically, choice behavior in EWA is governed by two key parameters capturing distinct computational components involved in updating players' action values and has been highly successful in explaining observations across a wide range of games at both behavioral and neural levels (*Materials and Methods*, Fig. S1, and Table S1). First, the belief learning parameter δ captures a player's sensitivity toward actions of opponents as opposed to received payoffs. An individual responding only to received payoffs is captured by $\delta = 0$, corresponding to a pure RL player, whereas a player driven entirely by belief learning is captured by $\delta = 1$. Using choice behavior and simulations for a single subject as illustration (Fig. 2*A*, *Upper*), a larger belief learning parameter is most saliently reflected in an increased probability of investing 2 and 3 in rounds 70–100, corresponding to periods when strong players invested 1–2 units with increased likelihood. Second, learning rate ρ governs how action values depreciate over time, capturing the degree to which players are sensitive to more recent observations relative to past ones. A player highly sensitive to recent observations, captured by a low ρ, will therefore adapt faster, for example during rounds 80–100 in Fig. 2*A*, *Lower*, whereas a player with a large ρ is similarly sensitive to recent and past observations and adapts more slowly.

Consistent with previous studies of strategic learning (4, 5), we found that the hybrid model significantly outperformed both reinforcement and belief-based learning models alone as measured using the likelihood ratio test ($P < 0.001$ for each) as well as the Akaike information criterion penalizing for number of parameters ($P < 0.001$ for each). To capture individual variation in behavior, we estimated a saturated (fixed effects) model where each participant was coded with individual belief learning and learning rate parameters, δ_i^S (mean = 0.36, SD = 0.17) and ρ_i^S

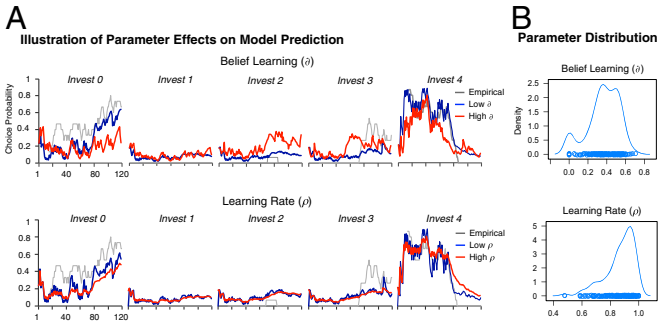

Fig. 2. (*A*) Illustration of parameter effects on model predictions using a single subject in the weak role. Actual subject choice behavior is presented as a time series smoothed using a 15-round bin average. Simulated choice probabilities were calculated using different belief learning and learning rate parameters. Each panel refers to a separate investment level. Note that a change in belief learning primarily affects the distribution of investment choices; in contrast, a change in the learning rate primarily affects the smoothness of adaption across rounds. (*B*) Density plot of individual-level belief learning (δ) and learning rate (ρ) parameters.

(mean = 0.86, SD = 0.10), respectively (Fig. 2*B*). This generated a set of individual-level belief learning parameters that we use in subsequent genetic analyses. Furthermore, we found that the individual estimates of the two parameters were largely uncorrelated (Spearman $\rho = 0.13$), which allowed us to characterize potential separable genetic contributions to behavior.

Characterization of Genetic Variation in Dopamine Pathway. We next sought to summarize variation of genes along the dopamine pathway. Using PCA and a 90% cutoff rule (*Materials and Methods*), we found SNPs within gene were highly correlated, consistent with nearby markers being in strong LD (Table 1). For example, four eigenSNPs contained 91% of the variation in the COMT gene, for which our genome-wide association (GWA) data contained 17 SNPs that exceeded a minor allele frequency (MAF) threshold of 0.1 (Table 1). Critically for our goal of identifying contribution of individual dopamine genes to behavior, we found using canonical correlation analysis that variation across genes are essentially uncorrelated (mean = 1.9 ± 1.4%; Table S2), consistent with distant marker being in weak LD.

Prefrontal Dopamine Genes Selectively Contribute to Variation in Belief Learning. Having summarized overall variation at both behavioral and genetic levels, we sought to identify genetic contributions to individual variation in the degree of belief learning, captured by the parameter δ. Specifically, for each gene in the dopamine pathway, we allowed the δ parameter in our computational model to vary according to the set of associated eigenSNPs, which can be interpreted as genetic variation that affects neural sensitivity to specific reward-related inputs (*Materials and Methods*). For example, in the case of the MAOB gene, in addition to the population parameter δ we included three additional parameters, $\{\delta_{E1},\delta_{E2},\delta_{E3}\}$, corresponding to the three eigenSNPs of the MAOB gene (Table 1 and *SI Materials and Methods*). Motivated by our previous neuroimaging findings suggesting PFC involvement in belief learning (5), we first examined genes known to regulate prefrontal dopamine levels. Specifically, we included the COMT gene and the two monoamine oxidase genes (MAO A and B) that code for isoforms of enzymes that break down extracellular dopamine. Functionally, MAOB is known to preferentially metabolize dopamine, whereas MAOA is more selective toward serotonin (18). Animal experiments using COMT knock-out mice suggest that MAO contributed to ∼20% of dopamine degradation, approximately half that of COMT (18).

Using permutation tests to assess the null hypothesis of no association, we found that allowing belief learning to vary according to COMT genotype significantly improved model fit (permutation $P < 0.005$, Table 1). In addition, and consistent with animal data on relative efficiency of the different enzymes in dopamine breakdown, we found that MAOB exerted a significant (permutation $P < 0.05$) albeit weaker influence on belief learning in terms of both significance as well as improvement in log likelihood (Table 1 and *Materials and Methods*). For MAOA, which has greater affinity to serotonin compared with dopamine (18), we found an even weaker association (permutation $P < 0.1$; Table 1). Interestingly, incorporating the 30-base repeat sequence VNTR, a highly studied polymorphism in the promoter region that has been implicated in behavioral traits such as aggression (19), together with SNP data significantly improved the model (permutation $P < 0.05$; Table 1). We then characterized genes that

Table 1. Summary of dopamine pathway genes and parameter estimates

						Belief learning (δ)				Learning rate (ρ)			
Function	Gene	SNPs	PCs	% Var	*k**	LLR	p_{unc}	p_{perm}	p_{emp}	LLR	p_{unc}	p_{perm}	p_{emp}
Synthesis	TH	2	2	100	1,089	0.98	0.374	0.898	0.888	0.9	0.400	0.913	0.932
	DDC	20	4	90	162	3.45	0.141	0.943	0.963	29.3	0.000	0.257	0.278
	VMAT2	16	8	92	22	31.1	0.000	0.420	0.410	12.3	0.002	0.969	1.000
Transport/clearance	DAT1	9	5	93	73	9.35	0.002	0.821	0.808	68.6	0.000	0.024	0.027
	VNTR					0.22	0.510	0.796		34.5	0.000	0.008	
	Joint					9.7	0.007	0.877		86.9	0.000	0.014	
	COMT	17	4	91	191	57.3	0.000	0.005	0.005	49.8	0.000	0.038	0.031
	MAOA	22	1	94	4	12.3	0.000	0.082	0.25	0.2	0.495	0.834	1.000
	VNTR					3.5	0.136	0.687		17.4	0.000	0.498	
	Joint					32.1	0.000	0.029		32.7	0.000	0.691	
	MAOB	28	3	95	70	32.7	0.000	0.035	0.029	1.2	0.000	0.585	0.586
Receptor	DRD1	5	3	99	275	9.22	0.000	0.522	0.510	9.76	0.000	0.639	0.647
	DRD2	17	5	94	159	24.8	0.000	0.295	0.296	67.5	0.000	0.036	0.025
	DRD3	6	3	97	289	2.49	0.174	0.881	0.917	23.9	0.000	0.219	0.201
	DRD4	1	1	100	975	3.40	0.009	0.335	0.396	9.46	0.000	0.193	0.183
	VNTR					11.9	0.000	0.247		12.5	0.000	0.314	
	Joint					12.0	0.000	0.398		25.8	0.000	0.207	

PCs, principal components; % Var, percent of total variance captured by included PCs; p_{unc}, *P* value using likelihood ratio test; p_{perm}, permutation *P* value (see *SI Materials and Methods*); p_{emp}, empirical *P* value (see *SI Materials and Methods*); TH, tyrosine hydroxylase; VMAT2, vesicular monoamine transporter 2.
*Number of matched comparison genes chosen from the GWA dataset.

primarily modulated striatal genes, as well as other genes in our dopamine pathway, including receptors and those involved in dopamine synthesis. In contrast, we did not find any of these to significantly improve model fit (minimum permutation $P <$ 0.30; Table 1).

Multiplexed Contribution of Dopamine Genes to Variation in Learning Rate. Next, we characterized genes that explained the other key parameter of our computational model—the learning rate ρ. As with the belief learning parameter, we allowed ρ to vary according the set of eigenSNPs in each dopamine gene. Motivated by our hypothesis that learning rate is primarily regulated by striatal functioning, we first characterized dopamine genes that disproportionately affected striatal dopamine functioning, in particular DAT1, and also dopamine receptor (DR) D2 and DRD3 (20, 21). We found that the DAT1 gene was significantly associated with variation in individual learning rates (permutation $P < 0.05$; Table 1). The existence of association is further enhanced by the fact that the DAT1 VNTR was also significantly associated with ρ (permutation $P < 0.01$; Table 1), as well as being jointly significant (permutation $P < 0.02$; Table 1).

Next we characterized dopamine receptor genes DRD2 and DRD3, which primarily affect dorsal and ventral striatal dopamine functioning, respectively. In previous neuroimaging results, activity in the dorsal striatum, in particular the putamen, but not the ventral striatum, was correlated with both reinforcement and belief prediction errors. However, there are reasons to suspect that the ventral striatum may also be involved, because it is widely implicated in neuroimaging studies on reward and decision making (22). We found that DRD2 was significantly associated with the learning rate (permutation $P < 0.05$), but not DRD3 (permutation $P > 0.2$; Table 1).

We then characterized genes that primarily affect prefrontal dopamine functioning. However, there are studies that suggest COMT exerts an indirect effect on striatal dopamine (23, 24). In contrast, we are not aware of human or animal studies demonstrating such indirect effects for MAO. Intriguingly, we found that COMT variation was significantly associated with the learning rate ($P < 0.05$), but not for either MAOA or MAOB ($P > 0.5$ for each; Table 1). Finally, we characterized dopamine synthesis genes as well as receptor genes that do not exhibit regional specificity and did not find that these genes are significantly associated with behavior (minimum $P = 0.19$; Table 1).

Distribution of Association Across the Genome. In the above results we have focused on permutation tests to guard against spurious associations compared with a random genotype. It is possible, however, that our evidence of association does not rise above the background association compared with the genome at large. To investigate this possibility, we compared the fit of models using dopamine genes relative to matching non-dopamine genes in the GWA dataset to generate an "empirical" null distribution (*SI Materials and Methods*). Strikingly, despite varying sizes of the comparison gene sets (Table S3), we found that the empirical null distributions, and consequently P values, tracked the permutation null closely in all dopamine genes tested (Table 1).

In addition, to formally compare effect size of prefrontal and striatal dopamine genes on choice behavior, we contrasted, using a bootstrap procedure, the mean eigenSNPs coefficient for COMT and MAOB against those for DAT1 and DRD2 (*SI Materials and Methods*). We found a strong dissociation between the two gene sets in the belief learning parameter δ, such that prefrontal genes exerted a significantly greater effect than striatal dopamine genes (bootstrap $P = .004$). In contrast, likely owing to the significant contribution of COMT to learning rate, we only found a weak dissociation in favor of striatal genes for the ρ parameter (bootstrap $P = .097$).

Mapping Genetic Variation to Behavioral Variation. Here we performed two types of model checks to illustrate how estimated genetic effects captured variation at the level of model parameters and choice behavior. First, to illustrate estimated genetic contribution to variation in the belief learning parameter δ, we imputed, for each individual, a gene-weighted parameter estimates δ_i^G by multiplying δ_{Ej} estimates with individual eigenSNP scores (*SI Materials and Methods*). Using these imputed parameters, we found that the variation in δ_i^G consistently reflected individual differences summarized by δ_i^S from the saturated model using fixed effects (Fig. 3*B*). For example, for the COMT gene, we found that the lowest quartile of δ_i^G estimates corresponded to a mean δ_i^S value of 0.26, compared with 0.45 for the highest quartile. Using the same procedure for the learning rate parameter ρ, we found a similar relationship with the gene-weighted parameter estimates ρ_i^G. For the DAT1 gene, for example, the lowest quartile of ρ_i^G estimates corresponded to a mean ρ_i^S value of 0.81, compared with 0.89 for the highest quartile (Fig. 4*B*).

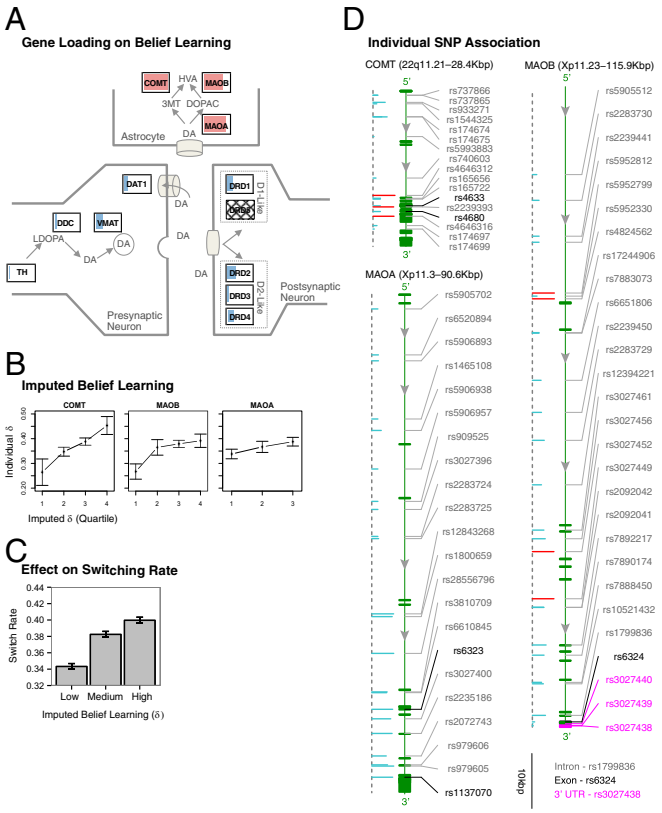

Fig. 3. (*A*) Permutation tests showed significant association of COMT and MAOB with individual variation in belief learning ($P < 0.005$ and $P < 0.05$, respectively), whereas MAOA was marginally significant ($P < 0.1$). No other genes were found to be significantly associated. Lengths of bars indicate likelihood improvement per principal component. Colors represent permutation P values. (*B*) To capture how genetic variation affects the degree of belief learning, we split, for each gene, the gene-weighted δ_i^G values into quartiles (terciles in the case of MAOA owing to limited genetic variation) and calculated the mean individual-level δ_i^F values (error bars are SEM). The former was calculated using the calibrated eigenSNP model, whereas the latter was estimated using fixed effects in a saturated model. (*C*) Effects of gene variation on switching rate were calculated as the probability that participants switched investment amounts between trials t and t+1, separated by the imputed gene-weighted learning parameter δ_i^G.Consistent with model predictions, individuals with higher δ_i^G values switched at a higher rate than those with lower values. (*D*) Individual SNP associations for belief learning parameter δ are shown on DNA strand. Thick green bands indicate exonic regions, purple bands UTRs, and otherwise intronic regions. Bar lengths indicate log-likelihood ratio (LLR) improvement, where red indicates significance at $P < 0.05$ and blue indicates nonsignificance. Scale is given at bottom right.

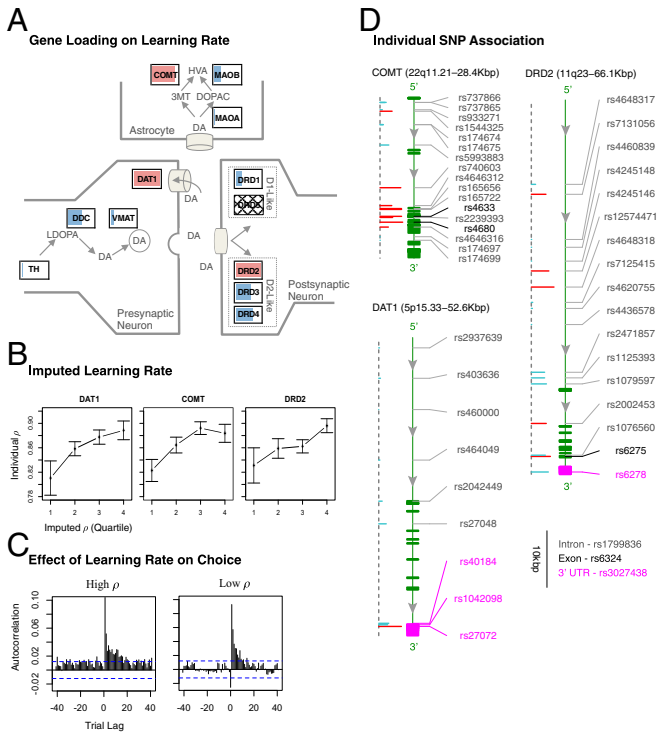

Fig. 4. (*A*) Permutation tests showed significant association of DAT1, DRD2, and COMT with individual variation in learning rate (all $P < 0.05$). Color coding and interpretation are identical to Fig. 3*A*. (*B*) To capture how genetic variation affects the learning rate, we split gene-weighted ρ_i^G values into quartiles and calculated the mean individual-level ρ_i^F values (error bars are SEM). (*C*) Effect of genetic variation on choice behavior is illustrated using correlogram of investment level at time t with payoff deviation at time $t\pm$ lag. The x axis represents different lags in number of rounds. Blue dashed lines indicate theoretical 95% confidence interval. Note the higher correlation values between periods 15–30 in high-ρ relative to low-ρ individuals. (*D*) Individual SNP associations for learning rate parameter ρ are shown on DNA strand. Color coding and interpretation are identical to Fig. 3*D*.

Next, we sought to quantify and visualize estimated genetic effects at the choice behavior level. First, as shown in previous theoretical and behavioral studies (4, 5), a key feature distinguishing belief and reinforcement learning is an increased rate of switching strategies across rounds by belief learners, owing to sensitivity of belief learners to the action of opponents (5). Consistent with this model prediction, we found that individuals with higher δ_i^G values indeed exhibited higher switching rates compared with those with lower values (Fig. 3*C*). Second, we sought to capture the influence of learning rate on choice behavior. Under EWA, individuals with lower ρ_i^G values should be influenced by more recent outcomes compared with those with higher values (4, 5). We therefore calculated a correlogram to measure how investment levels were influenced by payoff information at different lags (Fig. 4*C*). Consistent with model predictions, we found that for high ρ_i^G individuals past experiences continue to exert an effect well into 20 rounds in to the future, whereas for low ρ_i^G individuals this effect drops sharply after 10 rounds (Fig. 4*C*).

Distribution of Association Across SNPs. Next we sought to understand how identified behavioral effects are distributed across SNPs. Of SNPs in dopamine genes with a significant association with behavioral parameters, only one is associated with changes in protein sequence: rs4680 (Val158Met) in COMT, a polymorphism that causes changes in the catalytic activity of COMT and has been widely studied in the literature (Figs. 2*D* and 3*D*) (25). Seven other SNPs produce synonymous mutations that do not cause a change in the protein sequence. The vast majority of SNPs are located in intron sequences (60/79) or in the 3′ or 5′ UTRs of the target genes (11/79) (Figs. 3*D* and 4*D*). Furthermore, we computed the fit improvement for each SNP in the implicated genes (Figs. 3*D* and 4*D* and *SI Materials and Methods*). Consistent with the idea of multiple SNPs each exerting a weak influence on behavior, we observed that most SNPs exerted a small effect on our two learning parameters (Figs. 3*D* and 4*D*). We also explored the complementary notion that interactions between SNPs account for variation, finding qualitatively similar results (Table S4 and *SI Results*).

Discussion

There is now increasingly detailed knowledge of two physical substrates responsible for behavior: the brain and the genome (9). Here, we build upon these insights to shed light on the complex process by which genomic variation influences behavior through its impact on neural circuitry. Importantly, and similar to previous discussions in the computational neuroimaging literature, results from our computational approach should not be interpreted as an exercise to "localize Greek letters" in the genome (26). Just as it would be erroneous for neuroimaging researchers to interpret a particular brain region as a "prediction error module" or "a region encoding δ," in the same way it would be mistaken to interpret our results as suggesting that dopamine genes function as "belief learning genes" or "genes encoding δ." Rather, our goal is to test hypotheses regarding how variations in dopamine genes serve to constrain and regulate the computational properties of neural circuits subserved by dopamine.

More specifically, our results add to growing evidence that dopamine mechanisms critically underlie a wide class of value-based decision making across both social and nonsocial settings (11). They are consistent with a mechanism whereby neural computations related to the anticipation and response of actions of others are governed by dopamine genes involved in signal termination in PFC—primarily COMT and MAOA/B. Because prefrontal dopamine clearance mechanisms are slower than striatal, the PFC is thought to be sensitive to tonic, but not phasic, dopamine (27). This has led to the hypothesis that tonic prefrontal dopamine levels are important in maintaining active representations of relevant information and mediate learning after negative consequences (28). In our case, these functions might be relevant for maintaining a model of the partner's behavior and learning through belief-based prediction errors (5).

Furthermore, and in common with basic RL mechanisms, our results suggest that variation in proteins that affect dopamine signaling and clearance mechanisms in the striatum influence valuation of past experience in action selection. A possible mechanism proposed in the literature suggests that these variants modulate dopamine concentrations in meso-temporal scale (tens of milliseconds) by regulating phasic dopaminergic signaling in the striatum. In contrast, the effects of COMT on the learning rate is likely indirect and primarily operates through its effects on the balance of dopamine levels in frontostriatal circuits (23). In humans, these hypotheses can be tested indirectly by pharmacological manipulations on protein function (29).

At the molecular level, the explanatory power of polymorphisms not affecting protein structure raises the intriguing possibility that biochemical differences are caused by polymorphisms that do not directly affect protein sequence and function. For example, synonymous mutations in COMT have been shown to affect catalytic efficiency through regulation of translational efficiency (30). More generally, synonymous mutations are known to affect mRNA stability, transcriptional machinery binding affinity, and splicing, which can have significant consequences, as evidenced by the fact that they are often under selective pressure. UTR and intronic mutations, however, are likely to fall in upstream/downstream regulatory sequences where they could affect translation efficiency and protein levels (31).

Methodologically, we provide a tractable approach to connect gene and behavior by leveraging our knowledge of the intermediate

neural mechanisms. Unlike unconstrained hypothesis-free tests on individual polymorphisms, focusing on biological pathways allows us to relate systems of functionally related genes to putative mechanistic models of behavior. That is, we explicitly acknowledge the inherent tension regarding our current state of knowledge (8, 10). On the one hand, we now have an immense and growing base of knowledge regarding the biological basis of economic behavior, which can explain observation across multiple biological levels and, in some cases, across multiple species (3, 8). On the other hand, our knowledge is highly incomplete. Pathway analysis based on GWA data thus can complement these studies by testing multiple dopaminergic pathway genes for association with decision-making tasks rather than solely relying on an individual SNP approach (8, 10).

Taken together, these findings highlight the dissociable roles of dopamine genes in strategic learning and support the notion that variations in molecular mechanisms, organized along specific genetic pathways and brain circuits, form an important source of variation in complex phenotypes such as strategic behavior. More generally, these data suggest the intriguing possibility that, although complex phenotypes such as economic behavior are highly polygenic, the information is sparsely distributed across the genetic code and concentrated within specific functionally defined biological pathways.

Materials and Methods

Participants. A total of 218 (103 female) undergraduates were recruited from the Behavioral × Biological Economics and Social Sciences (B2ESS) Laboratory at the National University of Singapore. A total of 217 (103 female) were included in the final analysis after one subject was excluded owing to genotype unavailability (*SI Materials and Methods*).

Procedure. Participants completed 240 rounds of the patent race game in sessions of 18–24 participants, alternating between strong and weak roles over 120 rounds, counterbalanced. Informed consent was obtained as approved by the Internal Review Board at the National University of Singapore (*SI Materials and Methods*).

Genotype Selection and Preprocessing. For each dopamine gene (Fig. 1*B*), SNPs were included according to hg18 coordinates, and with MAF exceeding 0.1. DRD5 was excluded from the final analysis owing to lack of SNP variation in our sample. For details, including coding of VNTRs and X-chromosome genes, see *SI Materials and Methods*.

Computational Modeling. Denote s_i^k as strategy k (investment level) for player i, s_i (t) the chosen strategy by player i at period t, and $s_{-i}(t)$ the chosen strategy of the opponent at period t For each round, player i receives possible payoff $\pi_i(s_i^k, s_{-i}(t))$ for playing strategy s_i^k in period t, and the subjective value $V_i^k(t)$ for playing strategy k is governed by two parameters and updates according to the following:

$$V_i^k(t) = \begin{cases} \dfrac{N(t-1)\cdot\rho\cdot V_i^k(t-1) + \pi_i(s_i^k, s_{-i}(t))}{N(t)}, & \text{if} \quad s_i^k = s_i(t) \\ \dfrac{N(t-1)\cdot\rho\cdot V_i^k(t-1) + \delta\cdot\pi_i(s_i^k, s_{-i}(t))}{N(t)}, & \text{if} \quad s_i^k \neq s_i(t) \end{cases}, \qquad [1]$$

where $N(t) = \rho_i \cdot N(t-1)+1$ captures how $V_i^k(t)$ depreciates over time (for details, see *SI Materials and Methods*).

ACKNOWLEDGMENTS. We thank M. Monakhov, T. Rong, and X. Zhang for assistance in data collection. This research was supported by National Institute of Mental Health Grant R01 MH098023 (to M.H.), the Ministry of Education, Singapore (S.Z., R.P.E., and S.H.C.), and the AXA Research Fund (R.P.E. and S.H.C.).

1. Camerer C (2003) *Behavioral Game Theory: Experiments in Strategic Interaction* (Princeton Univ Press, Princeton).
2. Hofbauer J, Sigmund K (1998) *Evolutionary Games and Population Dynamics* (Cambridge Univ Press, Cambridge, UK).
3. Rangel A, Camerer C, Montague PR (2008) A framework for studying the neurobiology of value-based decision making. *Nat Rev Neurosci* 9(7):545–556.
4. Camerer CF, Ho T (1999) Experience-weighted attraction learning in games: A unifying approach. *Econometrica* 67(4):827–874.
5. Zhu L, Mathewson KE, Hsu M (2012) Dissociable neural representations of reinforcement and belief prediction errors underlie strategic learning. *Proc Natl Acad Sci USA* 109(5):1419–1424.
6. Behrens TEJ, Hunt LT, Woolrich MW, Rushworth MF (2008) Associative learning of social value. *Nature* 456(7219):245–249.
7. Hampton AN, Bossaerts P, O'Doherty JP (2008) Neural correlates of mentalizing-related computations during strategic interactions in humans. *Proc Natl Acad Sci USA* 105(18):6741–6746.
8. Ebstein RP, Israel S, Chew SH, Zhong S, Knafo A (2010) Genetics of human social behavior. *Neuron* 65(6):831–844.
9. Robinson GE, Grozinger CM, Whitfield CW (2005) Sociogenomics: Social life in molecular terms. *Nat Rev Genet* 6(4):257–270.
10. Wang K, Li M, Hakonarson H (2010) Analysing biological pathways in genome-wide association studies. *Nat Rev Genet* 11(12):843–854.
11. O'Connell LA, Hofmann HA (2012) Evolution of a vertebrate social decision-making network. *Science* 336(6085):1154–1157.
12. Schultz W, Dayan P, Montague PR (1997) A neural substrate of prediction and reward. *Science* 275(5306):1593–1599.
13. Pierce RC, Kumaresan V (2006) The mesolimbic dopamine system: The final common pathway for the reinforcing effect of drugs of abuse? *Neurosci Biobehav Rev* 30(2):215–238.
14. Nemoda Z, Szekely A, Sasvari-Szekely M (2011) Psychopathological aspects of dopaminergic gene polymorphisms in adolescence and young adulthood. *Neurosci Biobehav Rev* 35(8):1665–1686.
15. Frank MJ, Doll BB, Oas-Terpstra J, Moreno F (2009) Prefrontal and striatal dopaminergic genes predict individual differences in exploration and exploitation. *Nat Neurosci* 12(8):1062–1068.
16. Cortés R, Camps M, Gueye B, Probst A, Palacios JM (1989) Dopamine receptors in human brain: Autoradiographic distribution of D1 and D2 sites in Parkinson syndrome of different etiology. *Brain Res* 483(1):30–38.
17. Sauna ZE, Kimchi-Sarfaty C (2011) Understanding the contribution of synonymous mutations to human disease. *Nat Rev Genet* 12(10):683–691.
18. Shih JC, Chen K, Ridd MJ (1999) Monoamine oxidase: From genes to behavior. *Annu Rev Neurosci* 22:197–217.
19. Buckholtz JW, Meyer-Lindenberg A (2008) MAOA and the neurogenetic architecture of human aggression. *Trends Neurosci* 31(3):120–129.
20. Gainetdinov RR, Caron MG (2003) Monoamine transporters: From genes to behavior. *Annu Rev Pharmacol Toxicol* 43:261–284.
21. Missale C, Nash SR, Robinson SW, Jaber M, Caron MG (1998) Dopamine receptors: From structure to function. *Physiol Rev* 78(1):189–225.
22. Montague PR, King-Casas B, Cohen JD (2006) Imaging valuation models in human choice. *Annu Rev Neurosci* 29:417–448.
23. Dreher J-C, Kohn P, Kolachana B, Weinberger DR, Berman KF (2009) Variation in dopamine genes influences responsivity of the human reward system. *Proc Natl Acad Sci USA* 106(2):617–622.
24. Yacubian J, et al. (2007) Gene–gene interaction associated with neural reward sensitivity. *Proc Natl Acad Sci USA* 104(19):8125–8130.
25. Meyer-Lindenberg A, et al. (2006) Impact of complex genetic variation in COMT on human brain function. *Mol Psychiatry* 11(9):867–877.
26. O'Reilly JX, Mars RB (2011) Computational neuroimaging: Localising Greek letters? Comment on Forstmann et al. *Trends Cogn Sci* 15(10):450.
27. Garris PA, Wightman RM (1994) Different kinetics govern dopaminergic transmission in the amygdala, prefrontal cortex, and striatum: An in vivo voltammetric study. *J Neurosci* 14(1):442–450.
28. Frank MJ, Moustafa AA, Haughey HM, Curran T, Hutchison KE (2007) Genetic triple dissociation reveals multiple roles for dopamine in reinforcement learning. *Proc Natl Acad Sci USA* 104(41):16311–16316.
29. Pessiglione M, Seymour B, Flandin G, Dolan RJ, Frith CD (2006) Dopamine-dependent prediction errors underpin reward-seeking behaviour in humans. *Nature* 442(7106):1042–1045.
30. Nackley AG, et al. (2006) Human catechol-O-methyltransferase haplotypes modulate protein expression by altering mRNA secondary structure. *Science* 314(5807):1930–1933.
31. Chatterjee S, Pal JK (2009) Role of 5′- and 3′-untranslated regions of mRNAs in human diseases. *Biol Cell* 101(5):251–262.

Supporting Information

Set et al. 10.1073/pnas.1316259111

SI Materials and Methods

Participants. A total of 218 (103 female) undergraduates were recruited from the Behavioral × Biological Economics and Social Sciences (B2ESS) Laboratory at the National University of Singapore. All participants were of ethnic Han Chinese background and had undergone full genome sequencing. A total of 217 (103 female) participants were included in the final analysis after one subject was excluded owing to genotype unavailability.

Procedure. Behavioral data were collected from subjects playing the patent race game in 1-h sessions of 18–24 subjects. In the patent race game, programmed in zTree (1), two players take the role of firms competing to develop a new product. The product is worth a fixed prize and firms are given an endowment to invest. In the asymmetric version of the game we used, the prize is worth \$10 and the two players begin each round with endowments of \$5 and \$4 and are referred to as the "strong" and "weak" players, respectively.

Players can invest any integer amount from their endowment. The investments are subtracted from the potential earnings. To win the prize, one must invest strictly more than the opponent. For example, if the strong player invests \$4 and the weak player invests \$2, the payoff that round to the strong player is \$5 − \$4 + \$10 = \$11, whereas the payoff to the weak player is \$4 − \$2 = \$2. Players' endowments do not carry over from round to round, so the maximum investment available is always either four (for the weak type) or five (for the strong type).

At the beginning of each round, each player was randomly matched with a player of the other type. They played 120 rounds in each role, counterbalanced, for 240 rounds in total. They were fully informed of the rules and matching procedures. Compensation was equal to 10 Singapore dollars (SGD) plus either the average earnings per round or 7 SGD, whichever was higher.

To illustrate how players can anticipate and respond to the actions of others in this game, suppose the weak player observes the strong players frequently investing 5 units. He may subsequently respond by playing 0 to keep his initial endowment. Upon observing this, strong players can exploit the weak player's behavior by investing only 1 unit to obtain both the prize while keeping 4 units from the endowment. This may in turn entice the weak player to move away from investing 0 to win the prize. In contrast, pure reinforcement-learning (RL) players will respond to these changes in opponents' behavior in a much slower manner, because they behave by comparing received payoffs from past investments without consideration for the strategic behavior of others (2).

Genotyping. DNA was extracted from blood samples using QIAamp DNA Blood Midi Kit (Quiagen). SNP genotyping was performed at the Genome Institute of Singapore with HumanOmniExpress-12 v1.0 DNA Analysis Kit (Illumina Inc.). Over 730,000 genetic markers, primarily SNPs, across over 18,000 genes were collected from each subject.

All variable-number tandem repeats (VNTRs) were analyzed with PCR products loaded onto 1.5% (wt/vol) agarose gel with ethidium bromide, run for 1 h at 5 V/cm in Tris/borate/EDTA, and visualized in a UV camera.

The DRD4 exon III VNTR was analyzed with HotStar Plus DNA polymerase (0.3 U per reaction), 1× Q-solution, 1× CoralLoad buffer (Qiagen), 200 μM of each dNTP, 200 nM of each primer, and 10–20 ng of genomic DNA per reaction, in a volume of 10 μL. Primer sequences were as follows: forward 5′- GCGACTACGTGGTCTACTCG -3′, reverse 5′- AGGACCCTCATGGCCTTG -3′ (3). Thermal protocol included an activation step at –95 °C for 5 min, 40 cycles of 94 °C for 30 s, 55 °C for 30 s, 72 °C for 40 s, and final hold at 72 °C for 5 min.

The monoamine oxidase A (MAOA) VNTR was analyzed with PCR ReddyMix Master Mix (Thermo Fisher Scientific), 200 nM of each primer, and 10–20 ng of genomic DNA per reaction, in a volume of 10 μL. Primer sequences were as follows: forward 5′-ACAGCCTGACCGTGGA-3′, reverse 5′- GAACGGACGCTCCATT-3′ (modified from ref. 4). The thermal protocol included an activation step at –95 °C for 5 min, 35 cycles of 95 °C for 30 s, 58 °C for 30 s, 72 °C for 60 s, and final hold at 72 °C for 5 min.

The dopamine transporter (DAT) VNTR was analyzed with PCR ReddyMix Master Mix (Thermo Fisher Scientific), 100 nM of each primer, 0.2% DMSO, and 10–20 ng of genomic DNA per reaction, in a volume of 10 μL. Primer sequences were as follows: forward 5′- TGTGGTGTAGGGAACGGCCTG-3′, reverse 5′- CTTCCTGGAGGTCACGGCTCA-3′ (modified from ref. 5). The thermal protocol included an activation step at –95 °C for 5 min, 35 cycles of 95 °C for 30 s, 61 °C for 30 s, 72 °C for 30 s, and final hold at 72 °C for 10 min.

Gene Selection and Preprocessing. From the dopamine pathway defined in the Kyoto Encyclopedia of Genes and Genomes database, a manually curated collection of pathway maps widely used in gene-set analysis, we included dopamine genes that are involved in (*i*) dopamine synthesis [tyrosine hydroxylase (TH), dopa decarboxylase (DDC), and vesicular monoamine transporter (VMAT)], (*ii*) coding of dopamine receptors (DRD1–5; DRD5 was excluded from the final analysis owing to limited variation of SNPs in the sample), and (*iii*) dopamine transport and clearance [DAT1, catechol-*O*-methyl transferase (COMT), and MAOA/B]. For each gene, SNPs were included according to hg18 coordinates and had minor allele frequency (MAF) exceeding 0.1.

SNP extraction and filtering was conducted using PLINK (6) and snpStats (7). For each gene, SNPs were included if they were contained according to hg18 coordinates and had MAF exceeding 0.1. To reduce dimensionality of the genetic information, we represented each gene as a linear combination of orthogonal vectors using principle component analysis (PCA). Specifically, each analyzed gene is represented by a set of eigenvectors (eigenSNPs) (8) from principal components accounting for at least 90% of the total variation of that gene's SNPs. Occasional genotyping failures (less than 3% of all included SNPs had more than 2 out of 217 failures) were coded with the mean value of the SNP.

X-Chromosome Genes. Because MAOA/B genes reside on the X-chromosome, there is substantial uncertainty regarding the interpretation of allele scores across sex. We addressed this issue in two ways. First, we estimated the model separating sex. Second, we added a sex interaction term to account for multiplicative effects. Both yielded results similar to our original model.

SI Computational Modeling

Base Experience-Weighted Attraction Model (No Genes). Choice behavior was modeled using the hybrid model experience-weighted attraction (EWA) that has been widely used to characterize strategic learning (9). Denote s_i^k as strategy k for player i. Because strategies in the patent race are investments from either a \$5 or \$4 endowment, $k \in \{0, \ldots, 5\}$ when player i is strong and $k \in \{0, \ldots, 4\}$ when player i is weak. For period $t \in \{1, \ldots, 120\}$,

$s_i(t)$ is the amount invested by player i at period t, and $s_{-i}(t)$ is the chosen investment of the opponent at period t.

Player i's (possibly counterfactual) payoff at period t for some s_i^k, given the opponent's actual strategy $s_{-i}(t)$, is equal to the endowment less s_i^k, plus the \$10 prize if $s_i^k > s_{-i}(t)$. This potential payoff is denoted as $\pi_i(s_i^k, s_{-i}(t))$. Notice that, given $s_{-i}(t)$, this potential payoff differs from player i's realized payoff in period t except for when $s_i^k = s_i(t)$.

Player i's expected reward, $V_i^k(t)$, for playing strategy s_i^k in period t is governed by two parameters and updates according to the following:

$$V_i^k(t) = \begin{cases} \dfrac{N(t-1)\cdot\rho\cdot V_i^k(t-1) + \pi_i\left(s_i^k, s_{-i}(t)\right)}{N(t)}, & \text{if} \quad s_i^k = s_i(t) \\ \dfrac{N(t-1)\cdot\rho\cdot V_i^k(t-1) + \delta\cdot\pi_i\left(s_i^k, s_{-i}(t)\right)}{N(t)}, & \text{if} \quad s_i^k \neq s_i(t) \end{cases}, \qquad \textbf{[S1]}$$

where function $N(t) = \rho\cdot N(t-1) + 1$ captures the depreciation of $V_i^k(t)$. If the player believes his opponent is a fast adaptor, he will have a small ρ that depreciates past values faster. In contrast, δ captures the weight between foregone payoffs and actual payoffs when updating values. This corresponds to one of the key insights of the hybrid model that belief learning is equivalent to a model whereby actions are reinforced by foregone payoffs in addition to received payoffs as in RL models. Thus, δ can be interpreted as a psychological inclination toward belief learning (9). That is, the hybrid model reduces to the RL model when $\delta = 0$ and the belief learning model when $\delta = 1$.

To more concretely illustrate the effect of belief learning on behavior, we contrast an EWA strong player with $\delta_1 > 0$ with an RL strong player with $\delta_2 = 0$. Suppose our strong player i invests \$5 and the opponent invests \$1. Both for EWA and RL the value V_i^5 will update to take into account the realized payoff $\pi_i(5,1) = 10$. Unlike the RL player, however, the EWA player with $\delta_1 > 0$ will also update values associated with other actions, even if they were not chosen. For example, in this case the EWA player takes into account the hypothetical payoff $\pi_1(2,1) = 13$ (\$10 prize + \$3 saved from the endowment) based on the opponent's action. Note that as δ_1 increases the greater the sensitivity to the actions of the opponent, ultimately leading to a higher probability that \$2 will be invested in the next round relative to \$5.

Gene-Weighted Model. To account for gene variation, we allowed δ or ρ to vary according to the set of eigenSNPs or VNTR dummy variables. For example, in the case for the DAT1 gene, there were three eigenSNPs, and thus we replace the δ parameter in Eq. **S1** with the individualized term

$$\delta_i^G = \delta_0 + \delta_{E1}\cdot E_{i1} + \delta_{E2}\cdot E_{i2} + \delta_{E3}\cdot E_{i3},$$

where $\{E_{i1}, E_{i2}, E_{i3}\}$ refers to i's three eigenSNP scores and the associated parameters $\{\delta_{E1}, \delta_{E2}, \delta_{E3}\}$ refer to the coefficients on the eigenSNPs. The same procedure is followed for the ρ parameter. Note that this approach implicitly assumes a linear allele–dose–expression–response relationship. We relax this assumption in later analyses by allowing for SNP–SNP interaction.

Behavioral Data Analysis. To calibrate the models given subjects' behavior in the game, we estimated parameters of each model, including initial condition $N(0)$, using subjects' responses by maximizing the logistic log likelihood of the model predictions. To convert values into choices, we used a logit or softmax function to calculate the probability of player i playing strategy k in the next round, $p_i^k(t+1) = e^{\lambda\cdot V_i^k(t)} / \sum_{l=1}^{L} e^{\lambda\cdot V_i^l(t)}$, where λ is an estimated parameter capturing subjects' sensitivity to difference in expected reward associated with the different actions.

Using choice probabilities calculated from the softmax function, we performed maximum likelihood estimation with a grid search over a large range of values for all free parameters in all estimations, because the likelihood function is not globally concave. We aggregated observations conditional on the roles of the subjects and then fit the choice data by maximizing the log likelihood of the observed choices over rounds t for subject i. That is, $\sum_i \sum_t \log(p_i^{s_i(t)}(t))$. Maximum-likelihood estimation of parameters was performed using the quasi-Newton algorithm implemented in the fminunc function in MATLAB. Approximately 100 random or evenly spaced interior starting values were tried, all of which produced essentially identical estimates.

Individual SNP Analysis. We compare our gene-set methodology to other candidate gene approaches by analyzing a selection of individual SNPs for each of the significant genes. These SNPs were identified by cross-referencing the genetic markers available to us with the tagging SNPs suggested by the International HapMap Project's Generic Genome Browser (10). Appropriate tagging SNPs were determined based on pairwise correlations (11). For reference data, we used Han Chinese in Beijing in Data Rel 27 Phase II+III, Feb 09, on NCBI B36 assembly, dbSNP b126. R^2 and MAF cutoffs were 0.8 and 0.1, respectively.

SNP–SNP Interactions. To account for SNP–SNP interactions, we extended the eigenSNP approach by performing PCA on the set of regressors produced from a third-order interaction of the underlying SNP data. For example, if a gene contained 4 SNPs, we performed PCA on the set of 84 regressors, resulting from 4 original SNPs, an additional 16 second-order interaction terms, and a further additional 64 third-order interaction terms. Using the same procedure as outlined above, we took the set of eigenSNPs that explained at least 90% of the variance and included them in our computational model.

Permutation *P* Values. Under the permutation test null hypothesis, individuals are interchangeable, so label-swapping provides a new dataset sampled under the null hypothesis. In each permutation, therefore, the within-gene correlations are preserved and only the behavior–genotype relation is destroyed (6). For each gene, data were permutated 1,000 times by shuffling the gene–subject pairing. The reported P value is equal to the proportion of tests where model fit of the permuted dataset improved upon those of the original, unpermuted dataset.

Empirical *P* Values. Empirical P values were determined by comparing model fit of the gene within the dopamine pathway to comparison genes across the entire genome but outside of the dopamine pathway. A gene was considered comparable if (*i*) it was represented by the same or similar number of SNPs and (*ii*) these SNPs generated the same number of principal components according to the procedure outlined above. A range of SNPs was allowed in cases where an exact match produced too few genes (Table S1). This typically occurred when there were a large number of SNPs in the gene.

Formal Dissociation Test. To formally compare effect size of prefrontal and striatal dopamine genes on choice behavior, we contrasted, using a bootstrap procedure, the mean eigenSNP coefficients for COMT and MAOB against those for DAT1 and DRD2 (12). Specifically, for each of 1,000 iterations of the bootstrap we created a pseudosample by sampling with replacement behavioral and genetic data from 218 participants, and performed maximum likelihood estimates as described above. The resulting coefficients were standardized to ensure

comparability across eigenSNPs, and the reported P value is equal to the proportion of tests where the mean coefficient for one gene set was greater than that of the other gene set.

SI Results

Predictive Accuracy of EWA Model. To assess the ability of our model to capture choice behavior in the patent race, we compared actual proportion of investment against predicted investment proportion (Fig. S1*A*). This is equivalent to a scatterplot of the empirical and EWA prediction proportions as reported in Table S2. Each point represents an investment strategy, that is, strong investment of 5, separately for strong and weak roles. The predicted investment proportion was computed by averaging the round-by-round predictions of the baseline EWA model, aggregating all players over all 120 rounds. The dashed diagonal line represents perfect agreement between the model predictions and actual play. As evident from how closely each point lies to this line, model prediction and actual play are in good agreement, with a χ^2 test result of $P < 10^{-8}$ and a mean difference of less than 5%.

In addition, we sought to incorporate visualization of game dynamics by separating predictions into 30-round blocks, with blocks in the same sequence connected in a series (Fig. S1*B*). All points lie near the diagonal line, confirming the success of the hybrid model of capturing actual play at the finer temporal resolution. The successful modeling of the relative dynamics is also apparent in the generally diagonal pattern within each sequence of points. Although aggregating over rounds and subjects understates the full range of behavior, these plots make clear that the hybrid learning model performs well overall, including the capturing of movements where static approaches are not able to capture.

Note that we do not report a statistic such as R^2 because of the discrete nature of our dependent variable. This issue, as well as model checking techniques such as the one we report above, has been discussed in depth in both neuroimaging and neurophysiological studies of decision making (13).

Incorporating SNP–SNP Interactions. Owing to the low explanatory power of single SNPs, a frequent proposal is that there exists substantial variation that can be explained by accounting for SNP–SNP interactions (14). Accordingly, we investigated this question using our gene-set approach by conducting PCA on regressors formed using third-order interactions of SNPs within a gene (*SI Materials and Methods*). Using the same 90% cutoff rule, we found that incorporating SNP–SNP interactions improved model fit of genes that were previously significant, in particular COMT and DRD2 (Table S4). Interestingly, we did not find qualitative changes in overall level of significance of dopamine genes after accounting for SNP–SNP interactions.

1. Fischbacher U (2007) z-Tree: Zurich toolbox for ready-made economic experiments. *Exp Econ* 10(2):171–178.
2. Hopkins E (2002) Two competing models of how people learn in games. *Econometrica* 70(6):2141–2166.
3. Lichter JB, et al. (1993) A hypervariable segment in the human dopamine receptor D4 (DRD4) gene. *Hum Mol Genet* 2(6):767–773.
4. Sabol SZ, Hu S, Hamer D (1998) A functional polymorphism in the monoamine oxidase A gene promoter. *Hum Genet* 103(3):273–279.
5. Vandenbergh DJ, et al. (1992) Human dopamine transporter gene (DAT1) maps to chromosome 5p15.3 and displays a VNTR. *Genomics* 14(4):1104–1106.
6. Purcell S, et al. (2007) PLINK: A tool set for whole-genome association and population-based linkage analyses. *Am J Hum Genet* 81(3):559–575.
7. Solé X, Guinó E, Valls J, Iniesta R, Moreno V (2006) SNPStats: A web tool for the analysis of association studies. *Bioinformatics* 22(15):1928–1929.
8. Wang K, Abbott D (2008) A principal components regression approach to multilocus genetic association studies. *Genet Epidemiol* 32(2):108–118.
9. Camerer CF, Ho T (1999) Experience-weighted attraction learning in games: A unifying approach. *Econometrica* 67(4):827–874.
10. Gibbs RA, et al.; International HapMap Consortium (2003) The international HapMap project. *Nature* 426(6968):789–796.
11. de Bakker PI, et al. (2005) Efficiency and power in genetic association studies. *Nat Genet* 37(11):1217–1223.
12. Davison AC (1997) *Bootstrap Methods and Their Application* (Cambridge Univ Press, Cambridge, UK).
13. Sugrue LP, Corrado GS, Newsome WT (2005) Choosing the greater of two goods: Neural currencies for valuation and decision making. *Nat Rev Neurosci* 6(5):363–375.
14. Yacubian J, et al. (2007) Gene–gene interaction associated with neural reward sensitivity. *Proc Natl Acad Sci USA* 104(19):8125–8130.

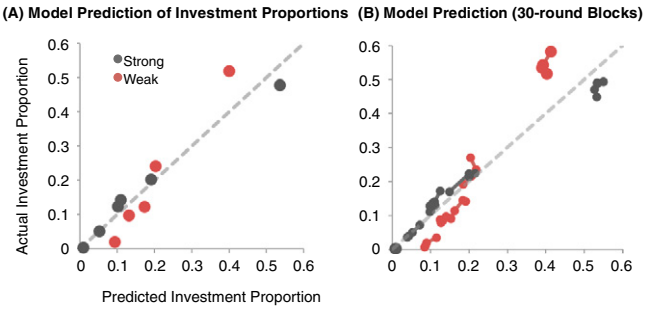

Fig. S1. (*A*) Predicted and actual investment proportions for strong and weak players, averaged over all subjects for all rounds. Each point represents an investment amount (weak, 0–4; strong: 0–5). (*B*) Identical to *A* except separated into 30-round blocks. Blocks are connected by series line.

Table S1. Empirical and predicted choice distributions, calculated as proportion of all players' choices over all rounds

Role	Investment	Nash equilibrium, %	Empirical distribution, %	Conditional win percentage, %	EWA prediction, %
Strong	0	0	0.4	0	0.9
	1	20	20.2	55	19.1
	2	0	5.1	57	5.2
	3	20	12.3	69	10.2
	4	0	14.3	77	11
	5	60	47.8	100	53.6
Weak	0	60	51.9	0	40.0
	1	0	2.0	0	9.4
	2	20	12.2	22	17.3
	3	0	9.7	27	13.1
	4	20	24.2	38	20.3

Table S2. Share of the variance of the gene that can be explained by another gene as calculated using the canonical correlation redundancy index (12)

Gene	COMT,%	DAT,%	DDC,%	DRD1,%	DRD2,%	DRD3,%	DRD4,%	MAOA,%	MAOB,%	TH,%	VMAT2,%
COMT	—	2.6	2.9	0.8	3.1	0.9	0.8	0.2	1.3	0.5	2.8
DAT1	2.1	—	2.3	1.2	2.0	1.9	0.9	0.4	1.6	1.0	3.6
DDC	2.9	2.8	—	1.3	2.5	1.6	0.8	0.8	1.4	1.5	3.2
DRD1	1.0	2.0	1.7	—	2.4	0.6	0.7	0.4	0.9	0.7	2.9
DRD2	2.5	2.0	2.0	1.5	—	1.4	1.1	0.7	1.9	3.0	4.3
DRD3	1.3	3.2	2.1	0.6	2.4	—	1.0	0.1	1.8	0.3	2.4
DRD4	3.2	4.6	3.2	2.0	5.4	3.0	—	0.1	2.1	1.0	1.6
MAOA	0.9	1.9	3.0	1.3	3.7	0.4	0.1	—	10.3	0.7	2.7
MAOB	1.7	2.7	1.8	0.9	3.2	1.8	0.7	3.4	—	1.5	1.5
TH	0.9	2.5	3.0	1.1	7.4	0.4	0.5	0.4	2.3	—	3.0
VMAT2	1.8	3.0	2.1	1.5	3.6	1.2	0.3	0.4	3.4	1.0	—

In the lower diagonal of the matrix, the row variable constitutes the dependent variable, and reversed for the upper diagonal. Note the only gene that explained 10% or more of the variance of another gene was the MAOB gene, which explained 10.3% of MAOA (which resides next to the MAOB gene on the X-chromosome) variation.

Table S3. Selection criteria for comparison genes outside of the dopamine pathway

Gene	SNPs	±
DRD1	5	0
DRD2	17	2
DRD3	6	0
DRD4	1	0
COMT	17	2
DAT1	9	1
MAOA	22	4
MAOB	28	6
TH	2	0
DDC	20	2
VMAT2	16	2

Table S4. Gene properties and estimates in SNP–SNP interactions

				Belief learning (δ)			Discounting (ρ)		
Function	Gene	PCs	% Var	LLR	p_{unc}	p_{perm}	LLR	p_{unc}	p_{perm}
Synthesis	TH	2	0.98	0.95	0.387	0.900	1.03	0.357	0.903
	DDC	8	0.91	21.75	0.000	0.737	28.86	0.000	0.73
	VMAT2	12	0.91	57.59	0.000	0.25	35.34	0.000	0.881
Transport/clearance	DAT1	5	0.91	12.98	0.000	0.646	70.17	0.000	0.019
	COMT	8	0.91	78.32	0.000	0.009	80.29	0.000	0.061
	MAOA	1	0.97	10.60	0.000	0.100	0.08	0.689	0.905
	MAOB	3	0.95	25.56	0.000	0.081	9.87	0.000	0.602
Receptor	DRD1	3	0.99	3.84	0.053	0.819	7.98	0.001	0.72
	DRD2	8	0.91	24.38	0.000	0.63	80.34	0.000	0.07
	DRD3	3	0.97	3.49	0.073	0.841	12.76	0.000	0.50
	DRD4	1	1.00	3.40	0.009	0.358	9.46	0.000	0.19

Owing to the low explanatory power of single SNPs, a frequent proposal is that there exists substantial variation that can be explained by accounting for SNP–SNP interactions. We investigated this question using our gene-set approach by conducting PCA on regressors formed using first-, second-, and third-order interactions of SNPs within a gene. Using a 90% cutoff rule as before, we found that incorporating SNP–SNP interactions improved model fit of a number of genes that were previously significant, particularly COMT and DRD2 (Table S3). However, we did not find that previously insignificant genes became significant after accounting for SNP–SNP interactions. PCA, principal component. % Var, percent of total variance captured by included PCs; LLR, log-likelihood ratio (compared to no-gene baseline); p_{unc}, *P* value using likelihood ratio test; p_{perm}, permutation *P* value (see *SI Materials and Methods*); p_{emp}, empirical *P* value (see *SI Materials and Methods*).